Title

Collaboration of human pickers and crop-transporting robots during harvesting – Part II: Simulator evaluation and robot-scheduling case-study

Authors

Seyyedhasani, Hasan
Peng, Chen
Jang, Wei-jiunn
et al.

Publication Date

2020-05-01

DOI

10.1016/j.compag.2020.105323

Peer reviewed

Collaboration of Human Pickers and Crop-transporting Robots during Harvesting - Part II: Simulator Evaluation and Robot-Scheduling Case-study.

Hasan Seyyedhasani[1,*], Chen Peng[1], Wei-jiunn Jang[1], and Stavros G. Vougioukas[1]

[1] Biological and Agricultural Engineering Department, University of California-Davis, One Shields Avenue, Davis, CA 95616
[*] Corresponding Author: Email: hshasani@ucdavis.edu; Tel.: +1 (859) 536 8233

ABSTRACT

Harvest-aid robots that transport empty and full trays during manual harvesting of specialty crops such as strawberries or table grapes can increase harvest efficiency, by reducing pickers' non-productive walking times. In Part I of this work, a modeling framework, and a stochastic simulator were presented for all-manual and robot-aided harvesting. This paper reports Part II of our work, which utilized data gathered in two strawberry fields during harvesting, to estimate the stochastic parameters involved in modeling pickers, and evaluate the prediction accuracy of the simulator for all-manual picking. Then, as a case study, non-productive time and harvest efficiency were estimated for robot-aided harvesting, for various picker-robot ratios and three priority-based reactive dispatching strategies for the robots. The simulator predicted the pickers' non-productive time during all-manual harvesting, with 6.4%, 3%, and 1.2% errors for the morning, afternoon, and "all-day" harvesting shifts, respectively. Statistical testing verified that predicted non-productive times followed the same distributions as the measured non-productive times (5% significance level). Simulations robustness was assessed by using morning data to simulate afternoon harvesting and vice-versa: non-productive times distributions were predicted accurately (10% significance level). Robot-aided simulation results – using the calibrated simulator for a 25-picker crew – showed that all-manual harvest efficiencies of 81.8% and 78.2% for morning and afternoon shifts increased to 92% and 86.5%, respectively, when five robots were deployed. Different scheduling policies did not affect efficiency when more than five robots were used, because there were always enough robots to serve pickers' requests immediately. Also, harvest efficiency plateaued when more than five robots were used, as a consequence of the time needed for a robot to travel to a picker.

Keyword: Specialty crops harvest mechanization; human-robot collaboration; multi-robot dispatching; harvest simulation.

1 INTRODUCTION

Labor for manual harvesting of open-field fresh market crops, like strawberries, blackberries and table grapes, contributes 55% (Bolda et al., 2016), 53% (Bolda et al., 2018) and 47.8% (Fidelibus et al., 2018) respectively, of the total operating cost per acre. In addition to labor cost, increasing farm labor shortages are driving the introduction of harvest mechanization (Charlton et al., 2019). Plant architectures and fruit sensitivity of the above mentioned crops do not allow for shake-catch mechanical harvesting approaches, such as those investigated for trellised apple trees (He et al., 2019). Furthermore, robotic harvester prototypes for such crops have not successfully replaced yet the perception, dexterity and speed of farmworkers, at a competing cost (Bac et al., 2014; Defterli, 2016). As an intermediate to complete mechanization, mechanical labor aids have been introduced. These machines can increase worker productivity by reducing workers' unproductive times. For example, orchard platforms eliminate the need for climbing ladders and walking to unload fruits in bins (Baugher et al., 2008). Autonomous vehicle prototypes have been developed to assist in bin management in orchards (Bergerman et al., 2015; Ye et al., 2017), to reduce the need for forklift operators. In strawberry production, mobile conveyors have been introduced to reduce the time pickers spend on walking, to get the produce from the plants to the designated loading stations and return to resume picking (Rosenberg, 2003). However, such conveyors are specific to strawberries and cannot be adapted to other crops. Furthermore, their adoption has been very slow, partly because of their high purchase cost, but mainly because the efficiency gains from their use can be limited. One reason for inadequate efficiency is that row-turning in the field is time-consuming because of their large size, but more importantly, because conveyors move slowly to accommodate slower pickers, often resulting in underutilization of faster pickers (Rosenberg, 2003).

As an alternative to large harvest aids, teams of small harvest-aid transports robots have been proposed and are being developed (USDA REEIS, 2013; Jang, 2018; Khosro Anjom & Vougioukas, 2019). These robots reduce pickers' walking and increase harvest efficiency, by providing human pickers with empty trays, and carrying filled trays to a collection station. Given that one tray-transport robot serves multiple pickers, i.e., it is a shared resource, proper scheduling of the robot team in real-time is essential, to minimize picker waiting times, and equivalently maximize labor savings and efficiency, in a cost-effective manner (Jang, 2018). Computing picker waiting times and harvest efficiencies for different robot scheduling algorithms, harvest scenarios (field size, crop load, crew) and robot teams (size, robot speeds, and capacities) requires validated models and simulators of manual and robot-aided harvesting.

Simulation has been used extensively to evaluate scheduling and routing algorithms for agricultural machinery executing field operations. Conceptually, the problem has been modeled in the context of operations research (Bochtis & Sørensen, 2010), and simulations have been developed for generic precision agriculture operations (Emi et al., 2013; Conesa-Muñoz et al., 2016a; Conesa-Muñoz et al., 2016b), and specific applications such as potato production (Zou et al., 2015); sugarcane harvesting (Santoro, Soler & Cherri, 2017); corn stalk cutting and anhydrous ammonia application (Seyyedhasani & Dvorak, 2018), large-scale seeding (Ahsan & Dankowicz, 2019). Also, workers' manual operations have been modeled in the context of tomato trellising and harvesting (Bechar, Yosef, Netanyahu, & Edan, 2007), sweet pepper harvesting (Elkoby, van't Ooster, & Edan, 2014), cherry harvesting (Ampatzidis, Vougioukas, Whiting, & Zhang, 2014), rose cultivation (van't Ooster, Bontsema, van Henten, & Hemming, 2015), and vineyard harvesting (Mesabbah, Mahfouz, Ragab, & Arisha, 2016).

Although farm worker activities and machine operations have been modeled separately, modeling and simulation of the collaboration of human pickers and transport robots in the context of harvesting has not been addressed. A methodology based on hybrid automata with stochastic parameters was developed and reported as Part I of this work by Seyyedhasani, Peng, Jang & Vougioukas (2019) to model the all-manual and robot-aided harvest and crop-transport operations. The model describes the picking and walking actions of human pickers and traveling and transport actions of robots, for specialty crops harvest operations. A finite state machine approach was adopted to model the discrete operating states of the agents (i.e., pickers and robots), including state transitions and interactions among human and robot states. Due to its foundation on hybrid automata, the model was developed to be used for harvesting simulation, but also to serve as an executable task model for robots to represent human actions, in the context of human-robot collaboration (Sheridan, 2016). Based on the developed model, a Monte-Carlo harvesting simulator was developed to sample the stochastic parameters from the corresponding frequency distributions and execute the hybrid automata that represent pickers, robots, and their interactions. The simulator integrated a robot scheduler module to evaluate different scheduling policies.

Given the model and simulation platform, the first goal of the work reported in this paper was to calibrate the Monte-Carlo strawberry harvesting simulator, and evaluate the prediction accuracies of the simulator's harvest efficiency metrics, based on real harvest data. The predicted picking efficiencies of the developed model and simulator were evaluated based on statistical analyses of ground truth data (worker walking speeds, picking speeds, and idle times) obtained from video footage of strawberry harvest operations; footage was obtained from several cameras that were dynamically positioned in the field during harvesting with a large crew of pickers. The second goal of this work was to utilize the simulator in a case study, and predict the waiting times and harvest efficiencies of a crew of strawberry pickers when transport robot teams of increasing sizes were deployed, and three different priority-based reactive scheduling strategies were used to dispatch robots.

The rest of the paper is organized as follows. Section 2 presents the methodology used to collect and process data to calibrate the harvesting simulator, and the three different reactive scheduling policies used in the case study. Section 3 presents and discusses the calibration experimental results and analyses of the calibrated simulator's prediction performance, and the results from using the calibrated simulator to predict the performance of robot-aided harvesting, under different scheduling policies and robot team sizes. Finally, section 4 summarizes the results and conclusions from this work and suggests possible future work.

2 METHODOLOGY

2.1 SIMULATION PLATFORM CALIBRATION

Within each defined state in the developed model, difference equations with stochastic parameters were used to model the agent motion and mass transfer during harvest and tray-exchanges between picking and transport agents. Stochastic parameters consisted of picker picking speed, V_P, picker walking speed to/back from the collection station, $\mathrm{V_W}$, picker travel speed between furrows, V_{T}, picker picking time, $\Delta\mathrm{t_{ef}}$, and picker idle time waiting at the collection station, Δt_{iq}. The distributions of the simulator's stochastic variables ($V_P, V_T, V_W, \Delta t_{ef}$, and Δt_{iq}) were estimated by monitoring the activities of 28 pickers during the harvest of two strawberry fields, in two consecutive days. The field experiments took place during the high-yield season, in the morning (06/28/2018) and afternoon (06/27/2018) to capture the performance of pickers in different ties, before and after their lunch breaks. The fields were in Santa Maria, California [34.9472, -120.524], [34.9477, -120.519], and covered approximately 2.58 ha and 2.56 ha respectively.

2.1.1 Data Collection Approach

The picker moving speeds and the picking times were estimated by: a) installing flags in the picking fields, before harvest, at known – measured – distances between them; b) video-recording the activities of the picking crew with digital cameras placed at appropriate locations, and c) having human observers (lab members) watch the videos with a timer to record the time intervals when pickers crossed consecutive flags.

Flag and Camera Placement

The raised beds in the field of study (Figure 1), were labelled for unique and easy identification, and flags were planted along the furrows - on the raised beds - prior to the start of harvesting. The distance between each pair of consecutive flags was 30 ft, and was measured using a measuring wheel. The terrain was flat and the wheel was moved slowly, so errors introduced by traversing uneven terrain and wheel slip were kept minimal (albeit not quantified). Five GoPro HERO6 cameras (GoPro Inc., San Mateo, CA, USA) were used to record picker activities. Camera #1 was deployed close to the collection station and recorded the tray delivery process (Figure 1a); cameras #2 and #3 were deployed inside furrows and recorded pickers' in-furrow activities (i.e., picking, transporting, and travelling) (Figure 1b); and cameras #4 and #5 were deployed in the field's headland and recorded pickers' in-headland activities (i.e., transporting and travelling), pickers' picking cycle (picking time and non-picking time), and pickers' transitions to the next furrow (Figure 1c).

Figure 1. Cameras deployed to monitor a) tray delivery process; b) in-headland activities, and c) in-furrow activities.

The cameras were set up (Figure 2) to collectively capture activities in a distinct region of interest (ROI), which was the most densely picker-populated area. Even though the horizontal field of view (hFOV) of camera #4 covered the ROI completely, camera #5 was deployed with significant hFOV-overlap to document the pickers' transition patterns from one furrow to the next. Footage examination revealed that after finishing a bed, pickers would almost always proceed to the closest unoccupied furrow associated with an unharvested bed. Unlike the headland cameras, the furrow cameras (#2 and #3) were complementary, so each of them covered half of the length of the ROI. After harvesting the beds in the ROI, the harvest crew moved on to the adjacent area of unharvested beds. The collection station also moved to pre-positioned positions (where empty trays had been stacked before harvesting) as the crew moved. Therefore, the cameras were also moved during harvesting to follow the crew activities in the new ROIs. In total, 40 hours of harvesting operation were recorded.

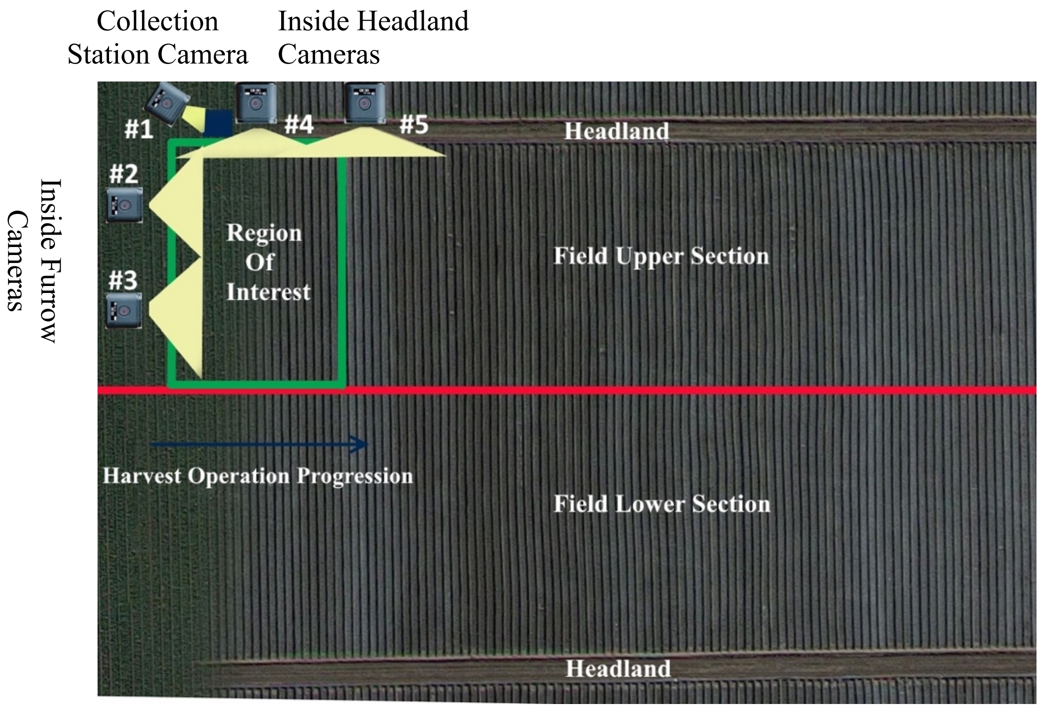

Figure 2. Layout of the field, the region of interest (ROI)where pickers harvested, and placement of the five cameras (#1 through #5).

2.1.2 Data Point Generation

Data points for the walking speed parameters ($V_P, V_W,$ and V_T) were estimated from the footage. The time instants t_0 and t_1 (Figure 3b) when a picker passed in front of two consecutive pre-positioned flags were recorded manually, with a timer. Given the known inter-flag distance in the field, d, the corresponding picker walking speed – for the corresponding discrete state - was computed as:

$$V = \frac{d}{t_1 - t_0} \tag{1}$$

As an example, the two frames (a, b) in Figure 3 *c*orrespond to t_0 and t_1 in the *PICKING* state, and were used to generate a single data point for parameter V_P. The curvilinear distortion of the camera lens or delays when the human observer clicks the timer may have introduced errors in the recording of the exact flag-crossing time instants, while viewing the footage.

a)

b)

Figure 3. Frames a and b correspond to t_0 and t_1, which are used to estimate a single data point for V_P in the PICKING state.

The estimation of data points for the picking time and idle-in-queue time parameters didn't rely on the flags, as the traversed distance was not relevant to the measurements. Picking time measurements (Δt_{ef}) were made by observing changes in a picker's body posture; such changes served as triggers for starting and stopping the timer. The time instants t_e when a picker with an empty tray bent over a bed (following a return from delivery), and the time instants t_f when (s)he stood up with the tray being full (to travel outwards a furrow for tray delivery) were recorded. The picking time was computed successive t_e, t_f measurements, as $\Delta t_{ef} = t_f - t_e$. The picker non-productive times Δt_{fe} were also computed by subtracting successive t_f, t_e measurements, as $\Delta t_{fe} = t_f - t_e$. The idle-in-queue times (Δt_{iq}) were measured by recording the successive time instants when a picker arrived with a full tray at the collection station and left with an empty tray.

2.2 Case-Study: Reactive Dispatching Strategies

As a case study, non-preemptive reactive robot dispatching for strawberry harvesting was considered, utilizing transport-robots with a capacity of one tray. The *Robot Scheduler* module prioritized requests using temporal (chronological order) or spatial (proximity) criteria. Three well-established heuristic policies were considered:

1) First Come First Served (FCFS): requests are served in the chronological order they arrive.
2) Shortest Processing Time (SPT): the request that is closest to the collection station - where the robots are stationed - is served first.
3) Longest Processing Time (LPT): the request that is farthest from the collection station is served first.

Both morning and afternoon harvesting operations were simulated for scenarios with 25 pickers and different sizes (*N*) of robot teams (i.e., $N = 2, 3, 4, 5, 6, 8$, and 10 robots). The robot speed was $V_r = 2\ ms^{-1}$, and the *TRAY-LOADING* state lasted $\Delta t_h = 5$ s. Each scenario was executed 100 times, and each run used random sampling of the stochastic parameters. The mean harvesting efficiency, $\overline{E}$, was computed as follows (Seyyedhasani, et al., 2019):

$$\overline{E} = \frac{\sum_{i=1}^{P}\sum_{j=1}^{n_i}\left(\Delta t_{ef}\right)_{ij}}{\sum_{i=1}^{P}\sum_{j=1}^{n_i}\left(\Delta t_{ef}\right)_{ij} + \sum_{i=1}^{P}\sum_{j=1}^{n_i}\left(\Delta t_{fe}\right)_{ij}} \tag{2}$$

where P is the size of the harvest crew, and n_i is the number of containers harvested by picker i. The mean and standard deviation of the waiting time ($\bar{t}_{wait}, \sigma_{t_{wait}}$) were computed from all trays of all pickers.

3 Results and Discussions

3.1 Frequency Histograms of Pickers' Stochastic Parameters

Figure 4 and Figure 5 present the frequency histograms of the pickers' stochastic parameters, $V_P, V_W, V_T, \Delta t_{ef}$, and Δt_{iq}, as these were measured from morning and afternoon harvest operations.

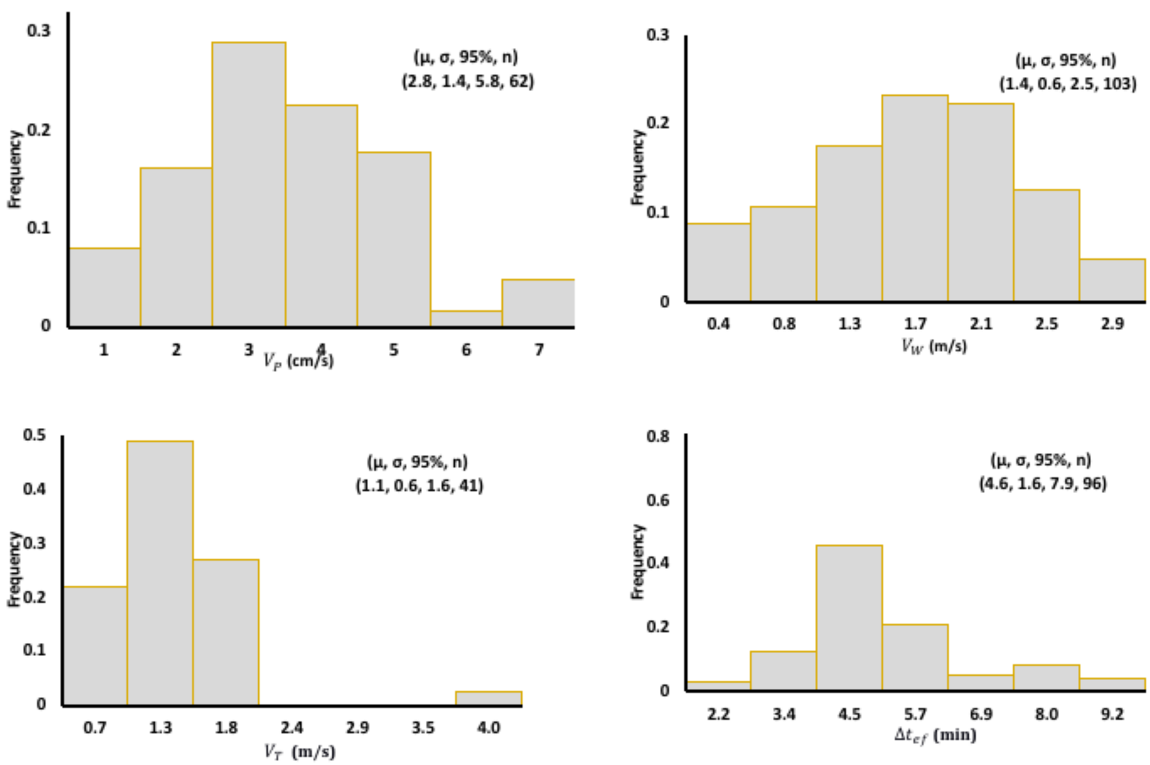

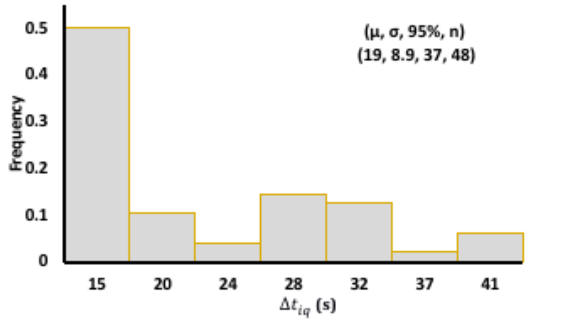

Figure 4. Frequency histograms of the pickers' stochastic parameters (morning harvesting); V_P: picker picking speed; V_W: picker walking speed to/back from the collection station; V_T: picker travel speed between furrows; Δt_{ef}*: picker picking time*; Δt_{iq}*: picker idle time waiting at the collection station.(*μ, σ, n*: mean, standard deviation, and number of data points, respectively)*

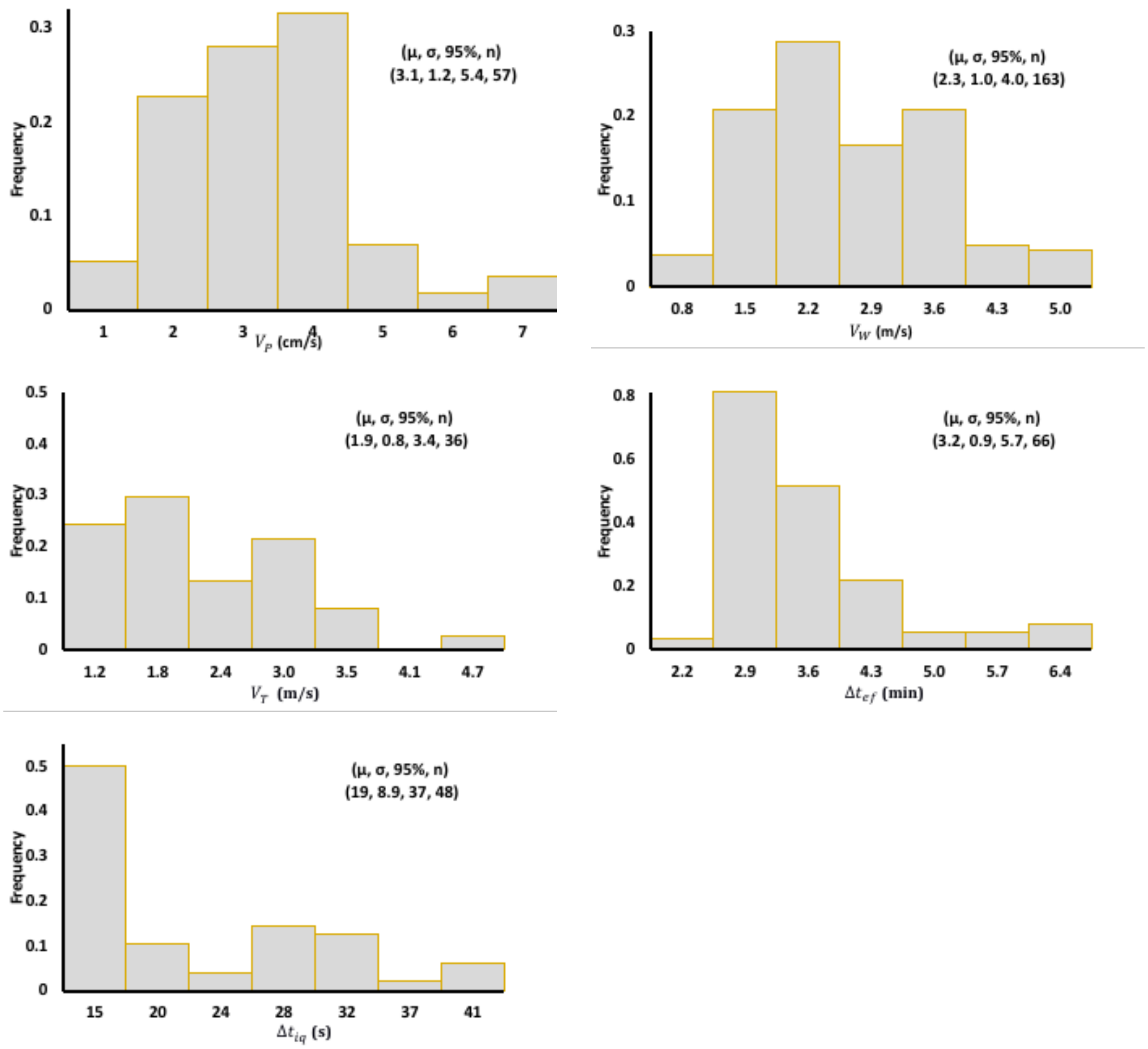

Figure 5. Frequency histograms of the pickers' stochastic parameters (afternoon harvesting); V_P: picker picking speed; V_W: picker walking speed to/back from the collection station; V_T: picker travel speed between furrows; Δt_{ef}*:*

picker picking time; Δt_{iq}: picker idle time waiting at the collection station.(μ, σ, n: mean, standard deviation, and number of data points, respectively)

The two-sample Kolmogorov-Smirnov (KS) and the two-sample t-test were used to compare the afternoon and morning distributions of each parameter, at the 5% significance level. The tests showed that the picking speeds V_P came from the same distribution, whereas V_W, V_T, and Δt_{ef} followed different distributions (Figure 6). Therefore, as a first step, the simulator was evaluated separately for morning and afternoon operations. In a second step, the evaluation was performed on the mixed/aggregated data from morning and afternoon, i.e., "all-day" harvesting.

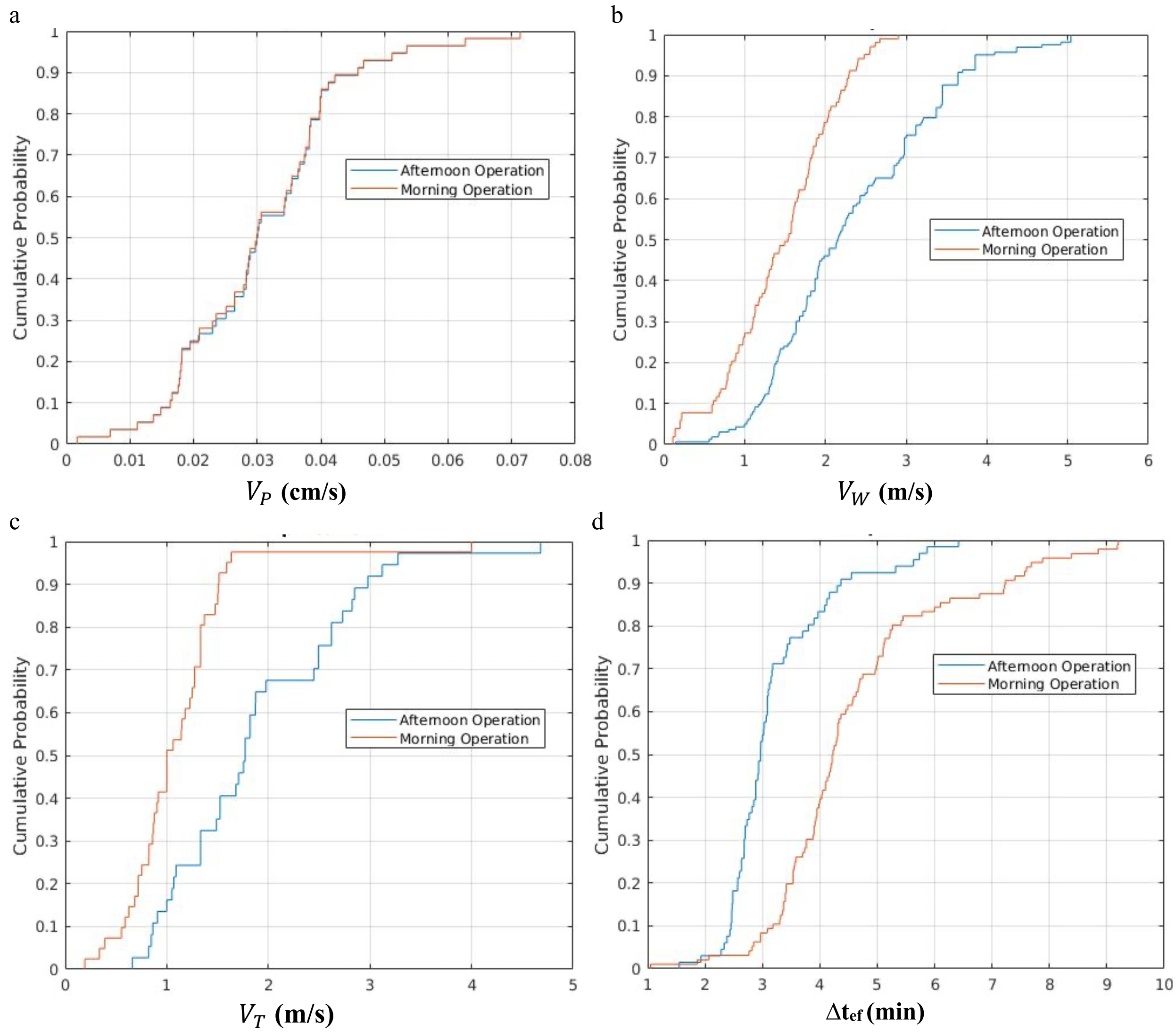

Figure 6. Cumulative probability distributions of the collected data from morning and afternoon harvesting: a) picker walking speed during picking, b) picker walking speed with empty tray, c) picker walking speed with full tray, and d) picking time;); V_P: picker picking speed; V_W: picker walking speed to/back from the collection station; V_T: picker travel speed between furrows; Δt_{ef}: picker picking time.

3.2 Evaluation of the Simulator

A total of 160 ground-truth data points were generated from the footage of the strawberry harvesting operations for the non-productive time Δt_{fe}. Table 1 contains some descriptive statistics. Δt_{fe} was significantly larger in the morning than in the afternoon. This can be partially attributed to the larger size of the field that was harvested in the morning, which resulted in pickers spending more time walking to deliver trays and moving to another bed. The standard deviations are large because Δt_{fe} involves walking time from field locations that may be very far from or very close to the collection station. As expected, the mean and standard deviation of Δt_{fe} for the mixed, "all-day" operation were between the corresponding values of the morning and afternoon operations, since it combined data from both. However, its standard error of the mean and 95% confidence interval were lower than those of morning and afternoon harvesting, because the calculation of these numbers involves a division by the total number of data points, which is bigger (160).

Table 1. Descriptive statistics of experimentally-derived Δt_{fe} (ground truth).

Operation Time	**# of Data Points**	**Mean Value of Δt_{fe} (s)**	**Standard Error of Mean Δt_{fe}**	**Standard Deviation (s)**	**95% Confidence Interval of Mean**
Morning	100	64.5	3.3	32.7	6.6
Afternoon	60	53.3	3.2	24.3	6.4
Mixed ("all-day")	160	60.3	2.4	30.2	4.8

The frequency histograms of Δt_{fe} are shown in the left column of Figure 7, for morning, afternoon and combined (all-day) harvesting; The right column of Figure 7 presents the corresponding histograms of the simulator-predicted $\widehat{\Delta t}_{fe}$.

a)

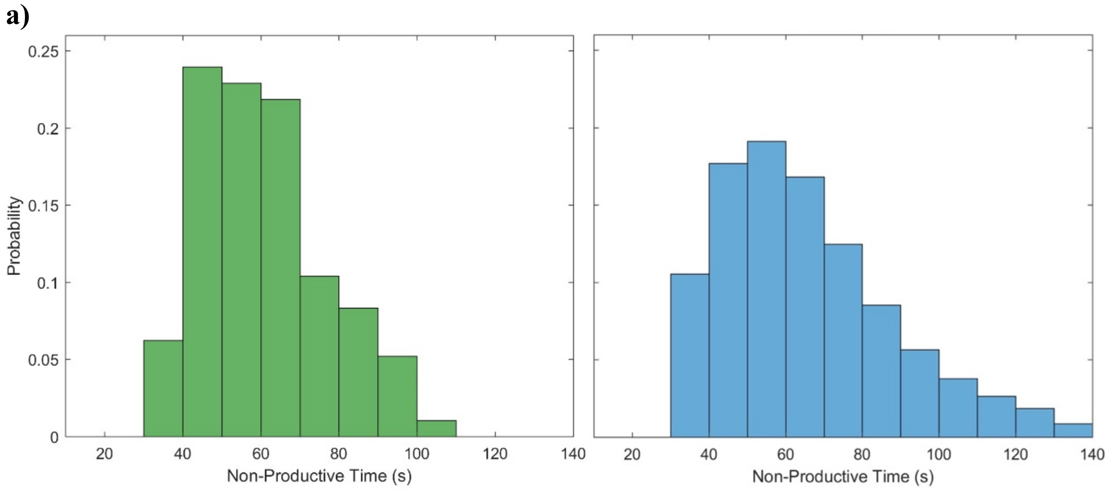

b)

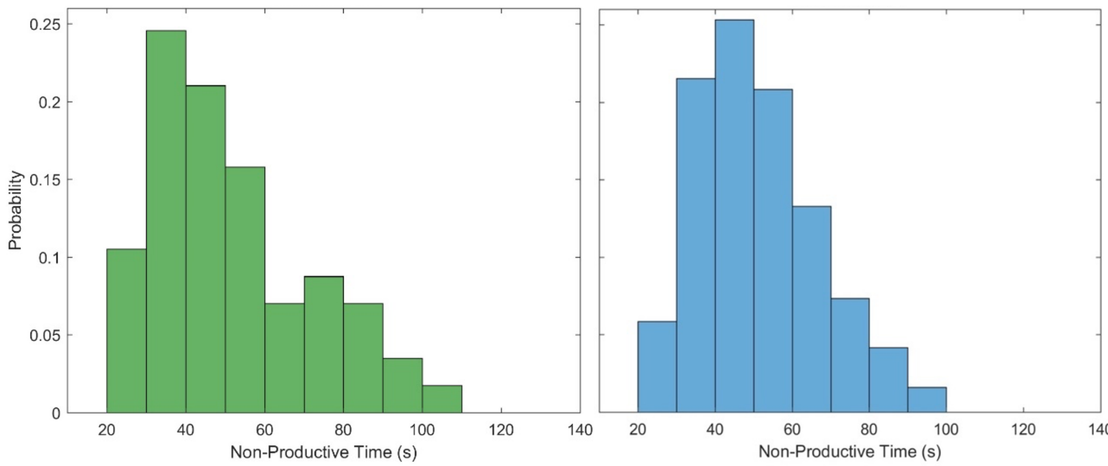

c)

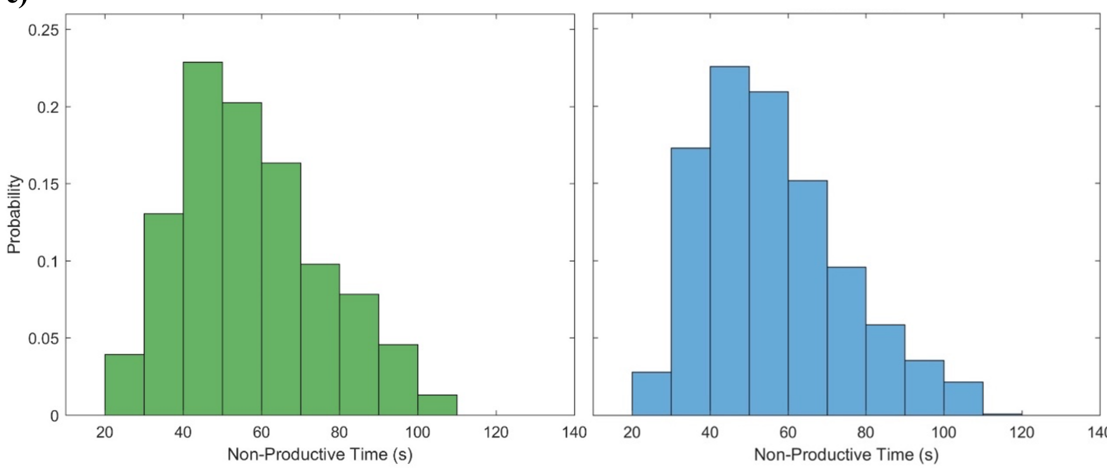

Figure 7. Frequency histograms of pickers' non-productive time during harvesting: a) morning, b) afternoon, c) mixed morning and afternoon operations. The left column (green bars) contains the measured non-productive times, Δt_{fe}, and the right column (blue bars) indicate the simulator-predicted non-productive times, $\widehat{\Delta t}_{fe}$.

Adopting as null hypothesis, H_0, that the distribution of $\widehat{\Delta t}_{fe}$ followed the distribution of the measured Δt_{fe}, the two-sample Kolmogorov-Smirnov test was performed on all operations, at 5% significance level. The test confirmed H_0 with p-values of 0.13, 0.66, and 0.21 for morning, afternoon, and mixed operations respectively (Figure 8).

a)

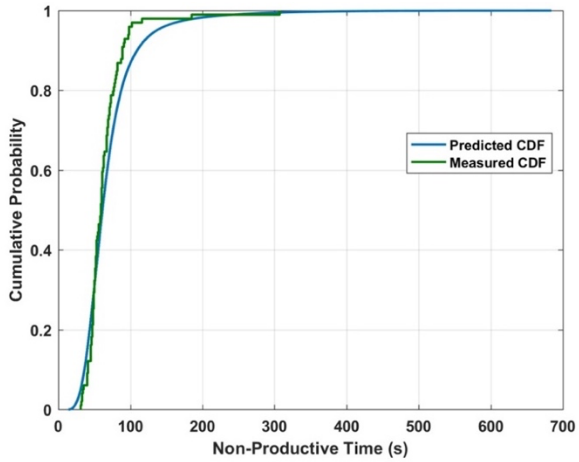

b)

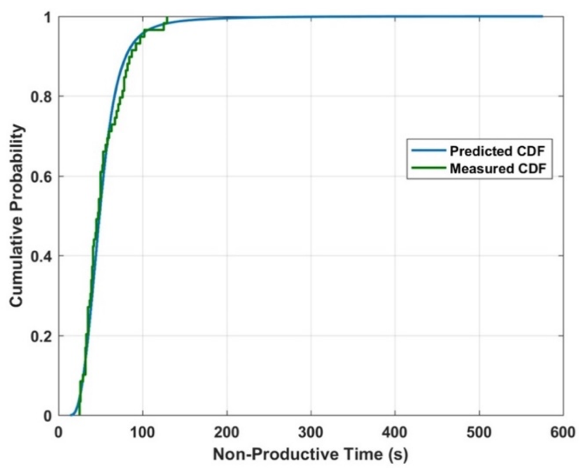

c)

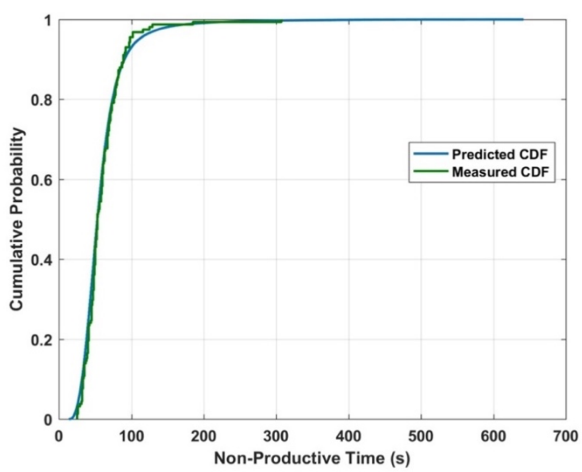

Figure 8. The measured and predicted cumulative distribution functions of a) morning, b) afternoon, c) mixed morning and afternoon operations

Table 2 presents the comparison between the ground truth non-productive times, Δt_{fe}, with the predicted ones, $\widehat{\Delta t}_{fe}$. The two-sample t-test showed that Δt_{fe} and $\widehat{\Delta t}_{fe}$ have equal means at 5%

significance level, with p-values of 0.17, 0.95, and 0.82 for morning, afternoon, and mixed operations, respectively.

Table 2.Comparison of pickers' measured and predicted non-productive times

Operation Time	Measured Δt_{fe}			Predicted $\widehat{\Delta t}_{fe}$	
	# of Data Points	**Mean Value (s)**	**Standard Deviation (s)**	**Mean Value (s)**	**Standard Deviation (s)**
Morning	100	64.5	32.7	68.6	41.6
Afternoon	60	53.3	24.3	54.9	26.9
Mixed (“all-day”)	160	60.3	30.2	59.6	33.8

The simulator predicted accurately the expected mean of the pickers’ non-productive time during manual harvesting, with errors of 6.4%, 3%, and 1.2% for morning, afternoon, and all-day harvesting respectively. The predicted $\widehat{\Delta t}_{fe}$ is overestimated in the morning because the parameter that affects $\widehat{\Delta t}_{fe}$ - picker walking speed with a full tray (V_W) - is *skewed toward lower values* (Figure 4; V_W skewness = -0.26) thus resulting in 6.4% larger simulated non-productive mean walking time. Afternoon walking speeds are *skewed toward higher values* (Figure 5; V_W skewness = 0.55) and the overestimate of the predicted $\widehat{\Delta t}_{fe}$ drops to 3%. The merged V_W data has slightly larger positive skewness = 0.65 and $\widehat{\Delta t}_{fe}$ is slightly underestimated (-1.2%).

To investigate the simulator’s *robustness* when the same crew picks at different places and times, the picker parameters of the morning operation in one field were used to predict the non-productive times of the afternoon operation in the other field, and vice versa. The null hypothesis was that Δt_{fe} and $\widehat{\Delta t}_{fe}$ followed the same distributions. The two-sample Kolmogorov-Smirnov test validated the null hypothesis in both cases, at the 10% significance level; the measured and predicted CDFs were $\pm 8\ s$ apart (Figure 9).

a)

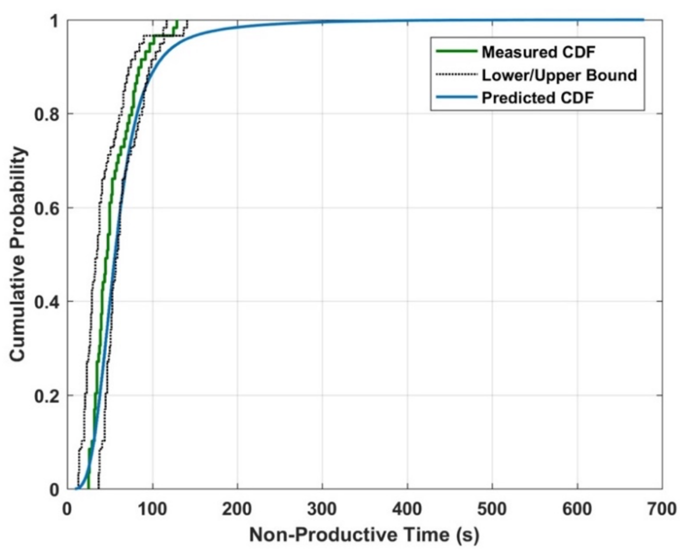

b)

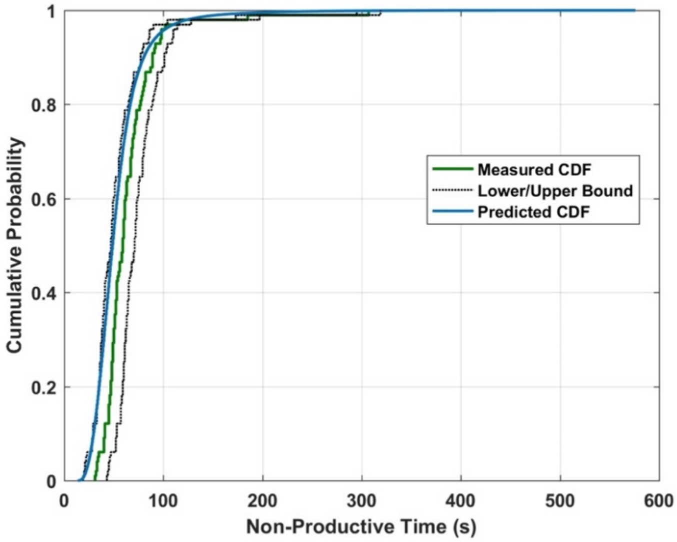

Figure 9. The measured and predicted cumulative distribution functions when a) the pdfs of morning operation predicted the non-productive time for afternoon operation and b) vice versa.

3.3 Case-Study: Reactive Dispatching Strategies

ERROR! REFERENCE SOURCE NOT FOUND. ERROR! REFERENCE SOURCE NOT FOUND.shows the statistics of the waiting times of twenty-five pickers served by robot teams of increasing size, *N*, during morning and afternoon harvesting.

Table 3. The statistics of the picker waiting time when twenty-five pickers are served by different numbers of robots during morning (a) and afternoon harvesting (b)

a

Number of robots *N*	FCFS Mean (s)	FCFS STD (s)	FCFS 95th Percentile (s)	SPT Mean (s)	SPT STD (s)	SPT 95th Percentile (s)	LPT Mean (s)	LPT STD (s)	LPT 95th Percentile (s)
2	222	88	370	227	1275	595	248	428	1232
3	71	46	160	66	131	198	78	118	287
4	32	21	73	30	30	70	34	34	81
5	24	12	45	24	14	45	24	15	44
6	21	10	39	21	10	39	22	10	39
8	21	9	36	20	9	36	21	9	37
10	20	9	36	20	9	36	21	9	37

b

Number of robots *N*	FCFS Mean (s)	FCFS STD (s)	FCFS 95th Percentile (s)	SPT Mean (s)	SPT STD (s)	SPT 95th Percentile (s)	LPT Mean (s)	LPT STD (s)	LPT 95th Percentile (s)
2	279	92	410	290	1973	465	1419	3898	1001
3	123	57	213	121	615	362	148	283	749
4	55	36	119	51	80	159	65	104	240
5	30	20	68	28	26	69	33	36	83
6	23	13	47	23	15	45	24	16	46

8	20	10	38	20	10	38	20	10	38
10	19	9	36	19	9	37	20	9	38

Regarding the effect of adding more robots, it was verified that, for all policies, the means, standard deviations and 95th percentiles of the waiting time followed closely ($R^2 > 0.99$) the power law $a \times b^N + c$, with $b < 1$. The fitted equations for morning harvesting are given in Table 4; results for afternoon harvesting are similar. The power law explains why the statistics of the picker waiting times improved dramatically as the number of robots, N, increased from two to three, regardless of the scheduling policy. The improvement continued further when 4 and 5 robots were deployed; however, it reached a plateau as the number of robots increased further. The reason is because the pickers' waiting time is lower-bounded by the distance between the collection station and picker location - at the point when the tray become full - divided by the robot travel speed. Even when at least one robot is always available for service, a picker has to wait for the robot to travel to him/her; this is a limitation of all reactive scheduling policies.

Table 4 Fitted power-law curves of the waiting time's mean value, its standard deviation and 95th percentile, for morning harvesting, for three harvesting policies (FCFS, SPT, LPT); results for afternoon harvesting are similar.

FCFS:	Mean	$3{,}245.29 \times 0.25^N + 20.37$;	RMSE=0.49 s
	Std.	$426.15 \times 0.44^N + 7.48$;	RMSE=1.77 s
	95th %	$2{,}583.37 \times 0.36^N + 33.20$;	RMSE=3.18 s
SPT:	Mean	$4{,}250.91 \times 0.22^N + 20.45$;	RMSE=0.59 s
	Std.	$138{,}294.97 \times 0.09^N + 11.59$;	RMSE=3.09 s
	95th %	$7{,}012.15 \times 0.28^N + 33.74$;	RMSE=4.11 s
LPT:	Mean	$3{,}647.00 \times 0.25^N + 20.76$;	RMSE=0.45 s
	Std.	$6{,}279.60 \times 0.26^N + 11.59$;	RMSE=1.07 s
	95th %	$27{,}616.33 \times 0.21^N + 35.06$;	RMSE=2.83 s

Regarding the effect of the different scheduling policies on waiting time, overall, LPT had the worst performance. When there were few robots (between two and five), the FCFS policy resulted in comparable values for the mean waiting time with the other two policies (with 3-5 robots, FCFS was slightly worse than SPT). However, the waiting time's standard deviation was much smaller for FCFS than for SPT and LPT. Standard deviation is related to *service consistency*, i.e., with FCFS scheduling, robot arrival delay times deviate less around the mean delay time. It is expected that pickers will prefer consistent service. When more than five robots were deployed, different scheduling policies did not introduce differences in the waiting time statistics, because there was always at least one available robot for each new tray transport request, so there was no need for prioritization.

The bar chart in Figure 10 depicts the mean of the harvest operation efficiency, $\overline{E}$, and its standard deviation, as more robots were deployed. The measured mean manual harvesting efficiencies were 81.8% and 78.2% for morning and afternoon harvesting, respectively. As the number of robots increased from 2 to 5, the mean robot-aided harvest efficiency improved from 55% to 92% for the morning operation, and from 41% to 86.5% for afternoon harvesting. Deploying 2, 3 or 4 robots to aid 25 pickers would make no sense, since their operation resulted in worse harvest efficiencies than all-manual harvesting. Deploying 5 robots increased harvest efficiency from 81.8% to 92% in the morning, and from 78.2% to 86.5% in the afternoon. There was marginal or no improvement when 6 or more robots were used, and efficiency peaked at 93.2% and 91% for morning and afternoon harvest, respectively. This was expected, since non-productive time plateaued also. The SPT, performed slightly better than FCFS, and consistently outperformed LPT. However, it caused significantly higher variance compared to the other dispatching policies, when utilized for deploying two or three robots (Figure 10). The standard deviation in picker efficiency decreased as more robots are deployed, with all policies.

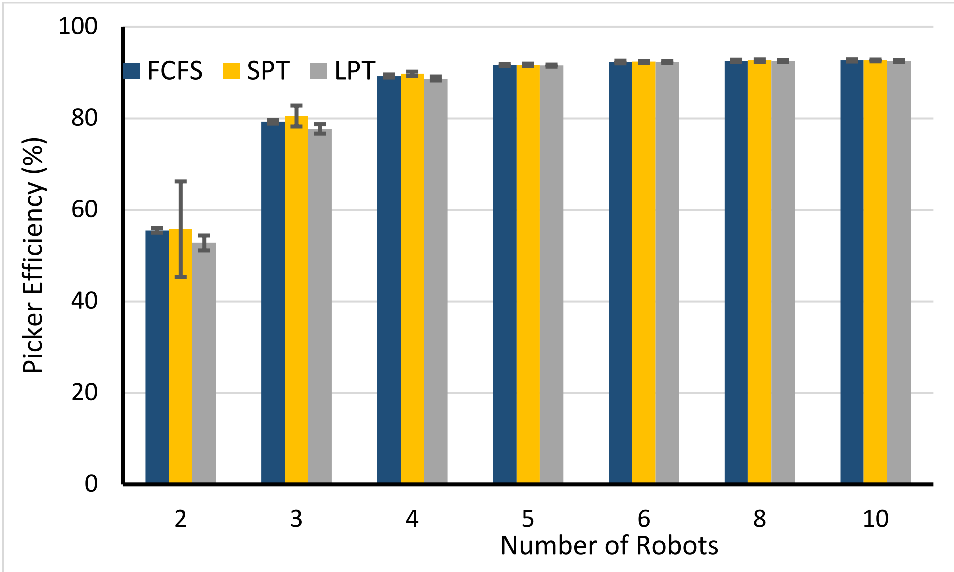

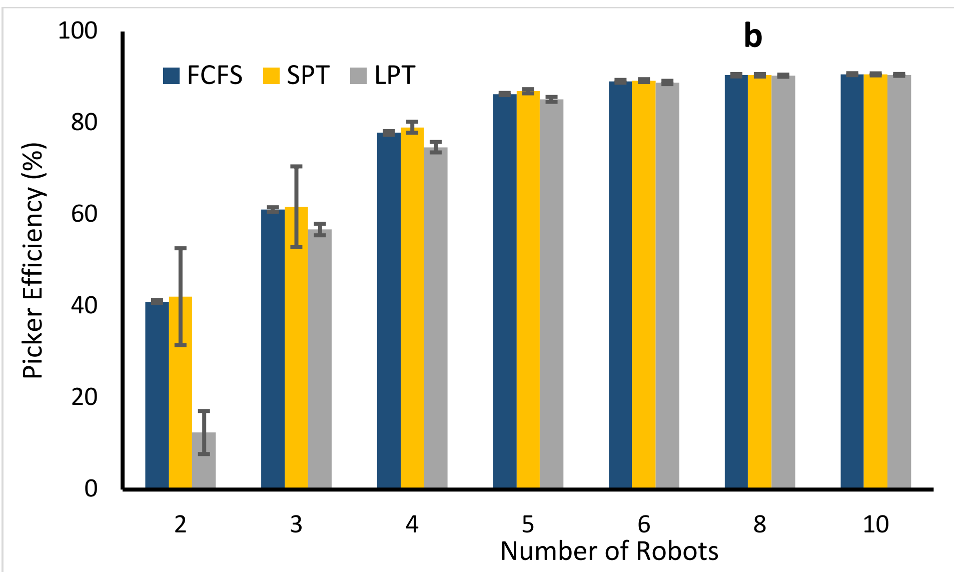

Figure 10. The pickers' mean efficiency and standard deviation when different number of robots are deployed during a) morning and b) afternoon operations

4 SUMMARY AND CONCLUSIONS

In Part I of this work, a model and a simulator were presented for robot-aided manual harvesting of specialty crops, with robots carrying empty and full trays, and workers performing the fruit picking. The picker model involved stochastic parameters. In the work presented in this paper, the distributions of the pickers' stochastic parameters were estimated from a crew of twenty-five pickers in commercial strawberry harvest operations. The calibrated simulator predicted the distribution of the non-productive time of the crew, with errors of 6.4%, 3%, and 1.2% for morning, afternoon, and all-day harvesting operations respectively. Also, statistical testing verified that the predicted non-productive times followed the same distribution as the measured non-productive times. As a case study, three reactive scheduling policies were implemented for the simulator's robot scheduler module: First-Come-First-Serve (FCFS), Shortest-Processing-Time (SPT) and Longest-Processing-Time (LPT). Overall, LPT had the worst performance.; serving distant pickers first, was not a good policy. With two robots available, the FCFS policy outperformed the SPT and LPT policies in reducing pickers' mean waiting time. When deploying 3, 4, or 5 robots, the SPT outperformed the other two scheduling policies; however, FCFS generated results with lower variance, resulting in more consistent service. Deploying five crop-transport robots enhanced the harvest efficiency up to 92% and 86.5% for morning and afternoon harvesting respectively, which was 81.8% for morning and 78.2% for afternoon manual harvesting. With more than five robots, the dispatching policies performed similarly, as there were always enough robots to serve pickers requests immediately. The mean harvest efficiency plateaued for more than five deployed robots, as a consequence of the mean travel distance that robots need to travel to get to a picker. Using more reactively-scheduled robots could not improve efficiency; predictive scheduling is one way to increase the harvest efficiency further.

The harvest efficiency– and efficiency increases - predicted by our methodology depend on the statistics of the operating parameters of the crew, which depend on picker performance, yield, field geometry and field and crop conditions. The data used in this work were collected in California during high-yield season, in a typical commercial strawberry field, with an experienced crew that was paid "piece-rate" (a fixed amount per hour plus an amount per harvested tray). However, the same methodology can be used to study manual and robot-aided harvesting in different settings, even with different crops (if they are picked similarly). Future work includes using the simulator to develop advanced – predictive – scheduling policies for the robots, and evaluating and comparing them for various crew-to-robot team size ratios. Also, transport robots are currently being developed and will be deployed in field experiments during commercial strawberry harvesting. Finally, detailed economic analysis will be conducted to assess under what conditions the introduction of such robots makes economic sense.

5 ACKNOWLEDGEMENTS

This work is part of the National Robotics Initiative project titled "FRAIL-bots: Fragile cRop hArvest-aIding mobiLe robots" that was funded by NIFA-USDA Grant 11423498, and by NIFA Hatch/Multi-State Grant 1001069. The UC Davis institutional review board (IRB) approval had been obtained for the study (protocol IRB 575389-5).

6 REFERENCES

Ampatzidis, Y. G., Vougioukas, S. G., Whiting, M. D., & Zhang, Q. (2014). Applying the machine repair model to improve efficiency of harvesting fruit. Biosystems Engineering, 120, 25-33.

Anjom, F. K., et al. (2018). "Development of a linear mixed model to predict the picking time in strawberry harvesting processes." Biosystems Engineering 166: 76-89.

Ahsan, Z. and Dankowicz, H., 2019. Optimal scheduling and sequencing for large-scale seeding operations. Computers and Electronics in Agriculture, 163, Article 104728.

Bac, C. W., Henten, E. J., Hemming, J., & Edan, Y. (2014). Harvesting Robots for High-value Crops: State-of-the-art Review and Challenges Ahead. *Journal of Field Robotics, 31*(6): 888-911.

Baugher, T., Schupp, J., Lesser, K., Harsh, R., Seavert, C., Lewis, K., Auvil, T. (2008). Mobile Platforms Increase Orchard Management Efficiency and Profitability. Acta Hort. (ISHS) 824:361-364.

Bechar, A., Yosef, S., Netanyahu, S., & Edan, Y. (2007). Improvement of work methods in tomato greenhouses using simulation. Transactions of the ASABE, 50(2), 331-338.

Bergerman, M., Maeta, S.M., Zhang, J., Freitas, G.M., Hamner, B., Singh, S. and Kantor, G., 2015. Robot farmers: Autonomous orchard vehicles help tree fruit production. IEEE Robotics & Automation Magazine, 22(1): 54-63.

Bochtis, D. and C. G. Sørensen (2010). "The vehicle routing problem in field logistics: Part II." Biosystems Engineering **105**(2): 180-188.

Bolda, M. P., Tourte, L., Murdock, J., & Sumner, D. (2016). Sample costs to produce and harvest strawberries. Available at https://coststudies.ucdavis.edu/current/. Accessed 15 August, 2019.

Bolda, M. P., Tourte, L., Murdock, J., & Sumner, D. (2018). Sample costs to produce and harvest fresh market blackberries. Available at https://coststudies.ucdavis.edu/current/. Accessed 15 August, 2019.

Charlton, D., Edward Taylor, J.E., Vougioukas, S.G., Rutledge, Z. (2019). Innovations for a Shrinking Agricultural Workforce. Choices, 2nd Quarter 34(2).

Conesa-Muñoz, J., Pajares, G., & Ribeiro, A. (2016a). "Mix-opt: A new route operator for optimal coverage path planning for a fleet in an agricultural environment." Expert Systems with Applications **54**: 364-378.

Conesa-Muñoz, J., Bengochea-Guevara, J. M., Andujar, D., & Ribeiro, A. (2016b). Route planning for agricultural tasks: A general approach for fleets of autonomous vehicles in site-specific herbicide applications. Computers and Electronics in Agriculture, 127: 204-220.

Defterli, S.G., 2016. Review of robotic technology for strawberry production. Applied Engineering in Agriculture, 32(3): 301-318.

D'Urso, G., Smith, S.L., Mettu, R., Oksanen, T. and Fitch, R. (2018). Multi-vehicle refill scheduling with queueing. Computers and electronics in agriculture, 144: 44-57.

Elkoby, Z., van't Ooster, B., & Edan, Y. (2014). *Simulation Analysis of Sweet Pepper Harvesting Operations.* Paper presented at the IFIP International Conference on Advances in Production Management Systems.

Emmi, L., Paredes-Madrid, L., Ribeiro, A., Pajares, G., & Gonzalez-de-Santos, P. (2013). Fleets of robots for precision agriculture: a simulation environment. Industrial Robot: An International Journal. **40**(1): 41-58.

Fidelibus, M., El-kereamy, A., Zhuang, G., Haviland, D., Hembree, K., Stewart, D. (2018). Sample costs to produce and harvest strawberries. Available at https://coststudies.ucdavis.edu/current/. Accessed 15 August, 2019.

He, L., Zhang, X., Ye, Y., Karkee, M. and Zhang, Q., 2019. Effect of shaking location and duration on mechanical harvesting of fresh market apples. Applied Engineering in Agriculture, 35(2): 175-183.

Jang, W. J. (2018). Investigation on the harvest-aid robot scheduling problem and the implementation of its simulation platform. Davis: University of California (M.Sc. thesis).

Jensen, M.F., Bochtis, D. and Sørensen, C.G., 2015. Coverage planning for capacitated field operations, part II: Optimisation. Biosystems Engineering, 139, pp.149-164.

Khosro Anjom, F., Vougioukas, S. G. (2019) Online Prediction of Tray-Transport Request Time for Robot-Aided Strawberry Harvesting using Mechanistic Grey Models. Biosystems Engineering. 188:265-287.

Mesabbah, M., Mahfouz, A., Ragab, M. A., & Arisha, A. (2016). Hybrid modeling for vineyard harvesting operations. In Proceedings of the 2016 Winter Simulation Conference (pp. 1642-1653). IEEE Press.

Patten, T., Fitch, R. and Sukkarieh, S., 2014, August. Multi-robot coverage planning with resource constraints for horticulture applications. In XXIX International Horticultural Congress on Horticulture: Sustaining Lives, Livelihoods and Landscapes (IHC2014): 1130 (pp. 655-662).

Rosenberg, H.R., 2003. Machine Aids in Strawberry Harvest: An Early Take on New Technology in Strawberry Harvesting. California Farmer, August 2003, pp. M1, 5, 9.

Santoro, E., Soler, E. M., & Cherri, A. C. (2017). Route optimization in mechanized sugarcane harvesting. Computers and Electronics in Agriculture, 141: 140-146.

Seyyedhasani, H. and J. S. Dvorak (2018). "Reducing field work time using fleet routing optimization." Biosystems Engineering **169**: 1-10.

Seyyedhasani, H., et al. (2019). " Collaboration of Human Pickers and Crop-transporting Robots during Harvesting - Part I: Model and Simulator Development." Computers and Electronics in Agriculture. Submitted.

USDA REEIS 2013. https://reeis.usda.gov/web/crisprojectpages/1000459-nri-small-frail-bots fragile-crop-harvest-aiding-mobile-robots.html. Accessed, August 1, 2019.

Van't Ooster, A., Bontsema, J., van Henten, E. J., & Hemming, S. (2012). GWorkS–A discrete event simulation model on crop handling processes in a mobile rose cultivation system. Biosystems Engineering, 112(2), 108-120.

van't Ooster, A., Bontsema, J., van Henten, E. J., & Hemming, S. (2015). Model-based analysis of skill oriented labour management in a multi-operations and multi-worker static cut rose cultivation system. Biosystems Engineering, 135, 87-102.

Ye, Y., Wang, Z., Jones, D., He, L., Taylor, M., Hollinger, G. and Zhang, Q., 2017. Bin-dog: A robotic platform for bin management in orchards. Robotics, 6(2):12.

Zhou, K., Jensen, A. L., Bochtis, D. D., & Sørensen, C. G. (2015). Simulation model for the sequential in-field machinery operations in a potato production system. *Computers and Electronics in Agriculture, 116*, 173-186.